Supplementary Figures

Fig. S1: Global and polar SAT pathways

Fig. S2: Seasonal and annual polar amplification during ramp-up

Fig. S3: Summer sea ice area trajectories across climate pathways

Fig. S4: Winter sea ice area trajectories across climate pathways

Fig. S5: Arctic winter: SIC temporal variability across stabilised and post-overshoot states

Fig. S6: Arctic summer: SIC temporal variability across stabilised and post-overshoot states

Fig. S7: Antarctic winter: SIC temporal variability across stabilised and post-overshoot states

Fig. S8: Antarctic summer: SIC temporal variability across stabilised and post-overshoot states

Fig. S9: Seasonal cycles of polar sea ice area and mass

Fig. S10: Matched-warming hysteresis in sea ice area

Fig. S11: Matched-warming hysteresis in sea ice mass

(a) Global mean.

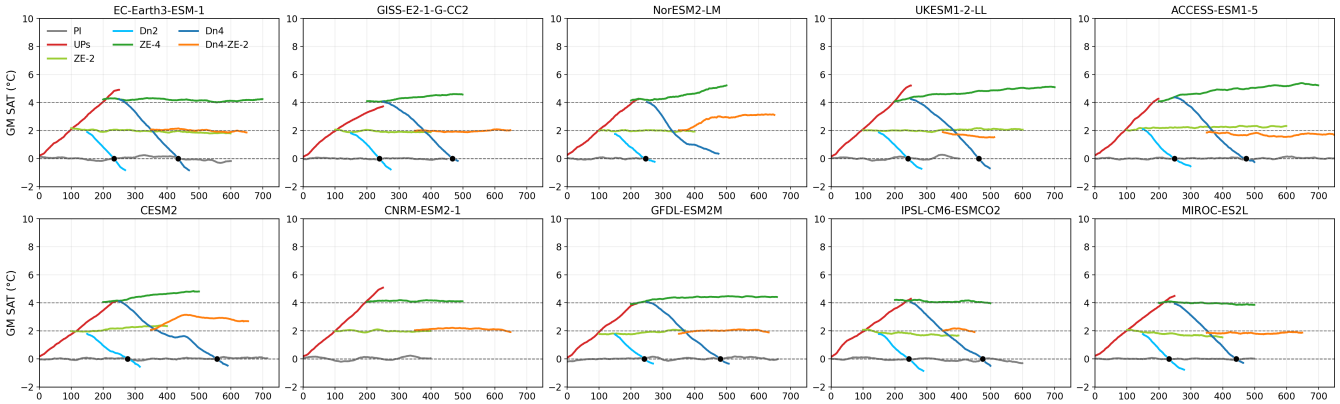

(b) Arctic region (60–90°N).

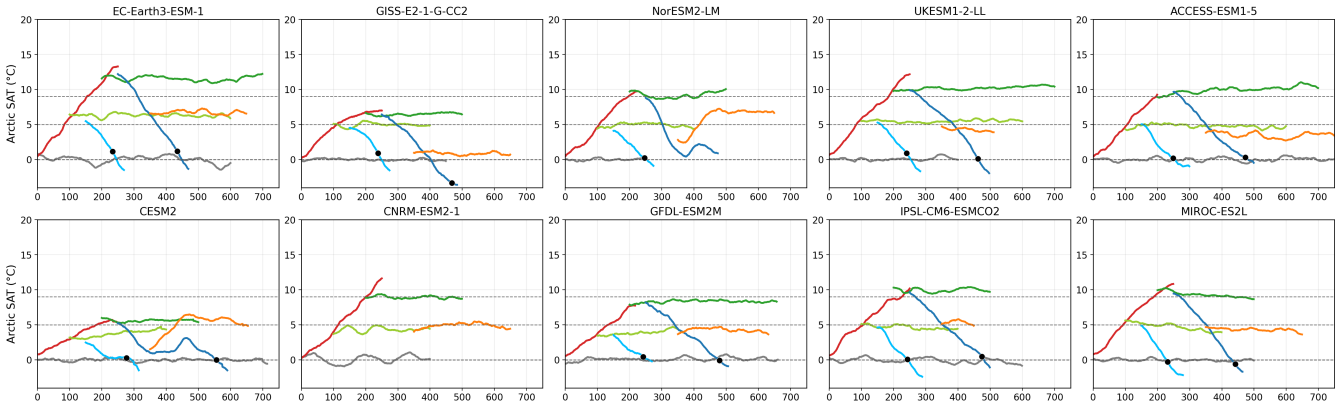

(c) Antarctic region (90–60°S).

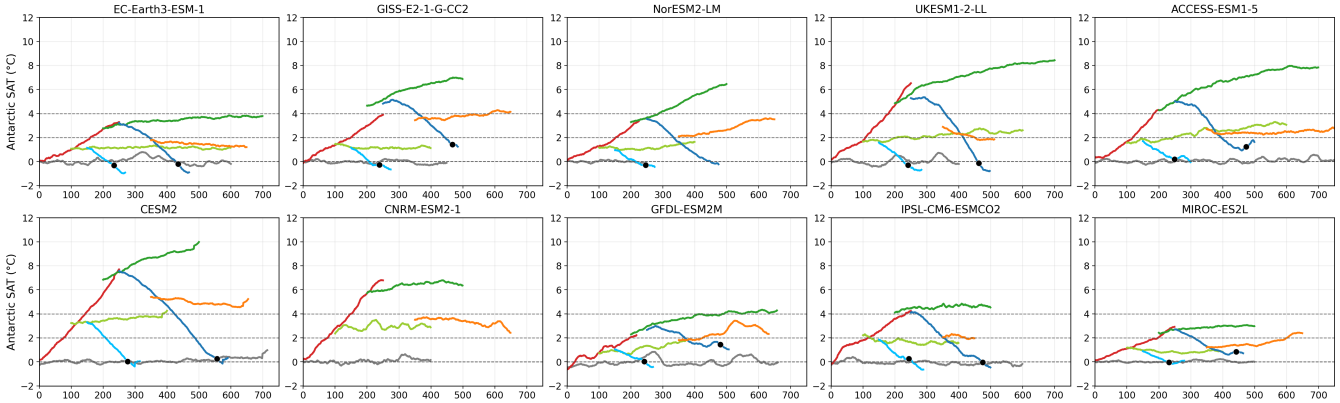

Figure S1. Global and polar SAT pathways for the TIPMIP Tier-1 model ensemble. Surface-air-temperature anomalies averaged over **(a)** the global domain (GM), **(b)** the Arctic region (60–90°N), and **(c)** the Antarctic region (90–60°S), after aligning the start years of the main experimental branches. Gray lines show the pre-industrial control (PI), red lines the ramp-up experiment (UPs; shown through aligned year 250 for visual consistency), light and dark green lines the zero-emission at GWL=2 and 4 °C experiments (ZE-2 and ZE-4), light and dark blue lines the ramp-down experiments from GWL=2 and 4°C (Dn2 and Dn4), and orange lines the zero emissions after cooling from 4 to 2 °C GWL (Dn4-ZE-2). Black dots mark when GMSAT returns to this reference during Dn2 and Dn4; NorESM2-LM Dn4 shows no clear return to GWL=0°C, and CNRM-ESM2-1 has no Dn2 or Dn4 simulations.

(a) Arctic region (60–90°N).

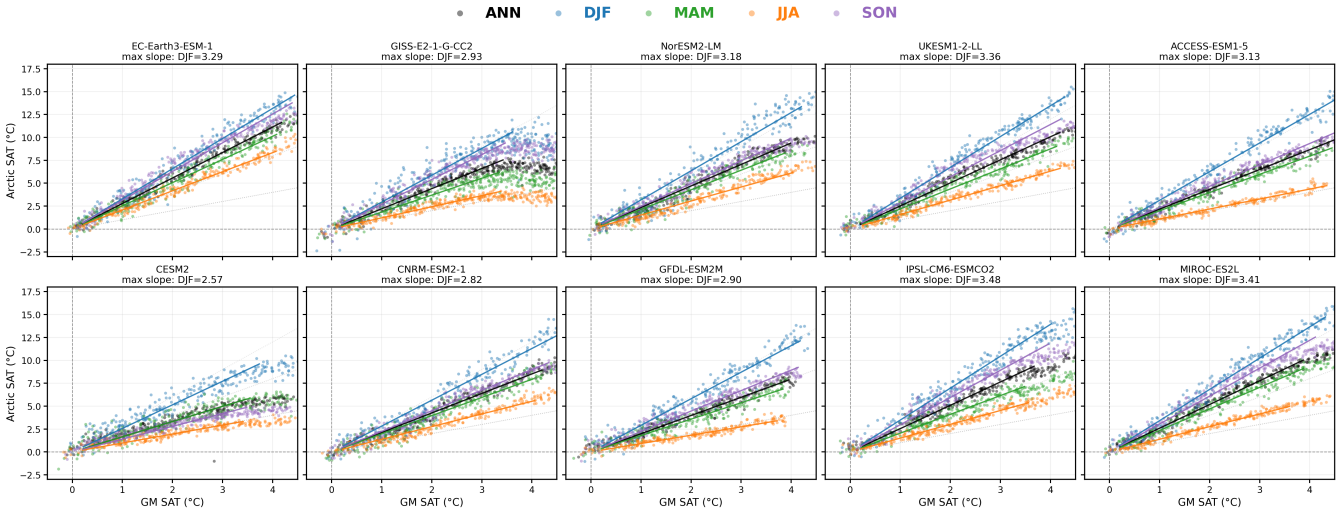

(b) Antarctic region (90–60°S).

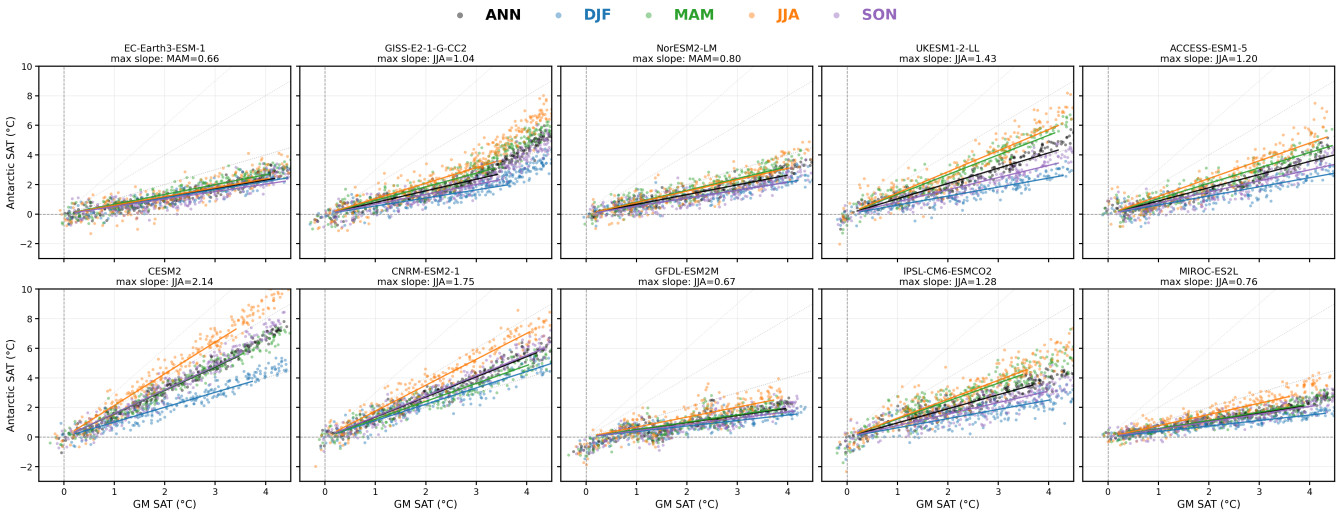

Figure S2. Seasonal and annual PA during ramp-up. Annual (ANN) and seasonal SAT anomalies over: **(a)** the Arctic region (60–90°N), and **(b)** the Antarctic region (90–60°S), plotted against the corresponding GMSAT anomalies during the ramp-up experiment (UPs). ANN is black; seasons are coloured. Points show annual values and the fitted slopes quantify the seasonal PA over the first 200 ramp-up years. The season with the largest fitted slope is indicated above each model panel. At high GWLs, some models show nonlinear Arctic winter temperature responses, including a weakening of the fitted amplification associated with strongly depleted winter sea ice (Fig. S4). However, this high-warming nonlinearity occurs only in a subset of models that reach sufficiently large GMSAT anomalies, and therefore should be interpreted as model-dependent threshold-like behaviour rather than a common ensemble threshold.

(a) **Arctic sea ice area in September.**

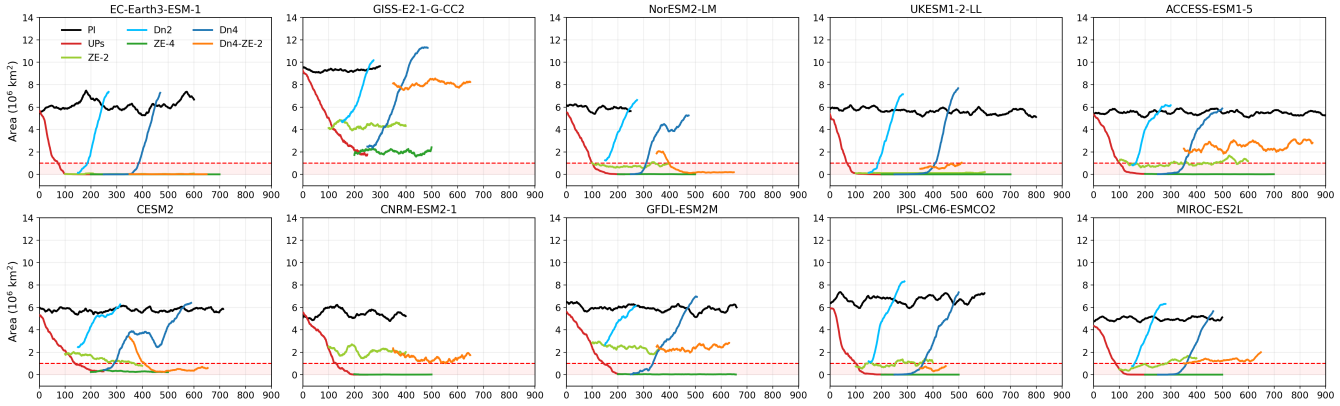

(b) **Antarctic sea ice area in March.**

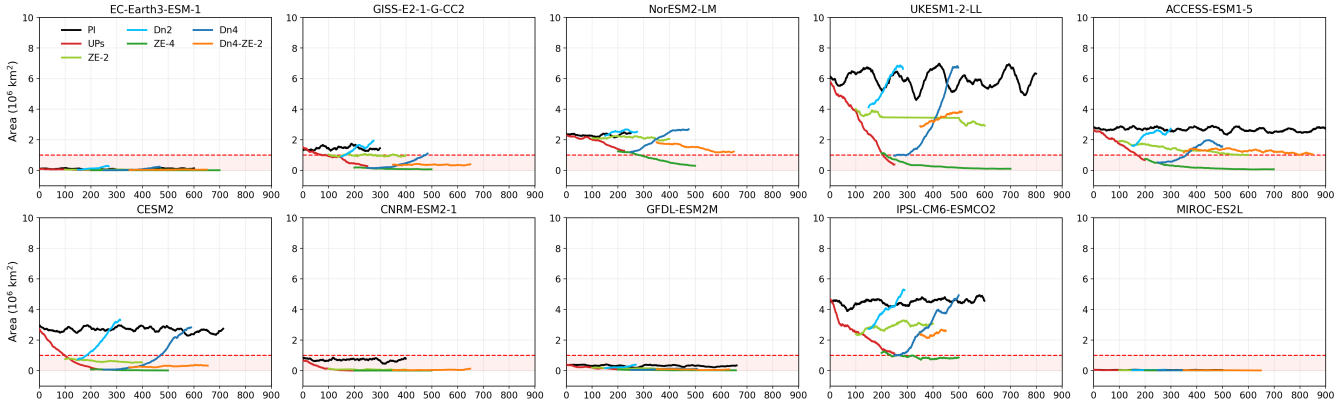

Figure S3. Summer sea ice area across TIPMIP climate pathways. (a) September Arctic sea ice area and (b) March Antarctic sea ice area for individual models across the UPs, ZE-2, ZE-4, Dn2, Dn4 and Dn4-ZE-2 experiments. See Fig. S1 for experiment definitions. Curves show 31-year running means, while the horizontal dashed line marks 1×10^6 km^2. For September, this threshold denotes an ice-free Arctic; for March, the same threshold is used as a diagnostic of near-complete sea ice loss rather than a conventional Antarctic ice-free definition. UPs is shown through aligned year 250 for visual consistency.

(a) **Arctic sea ice area in March.**

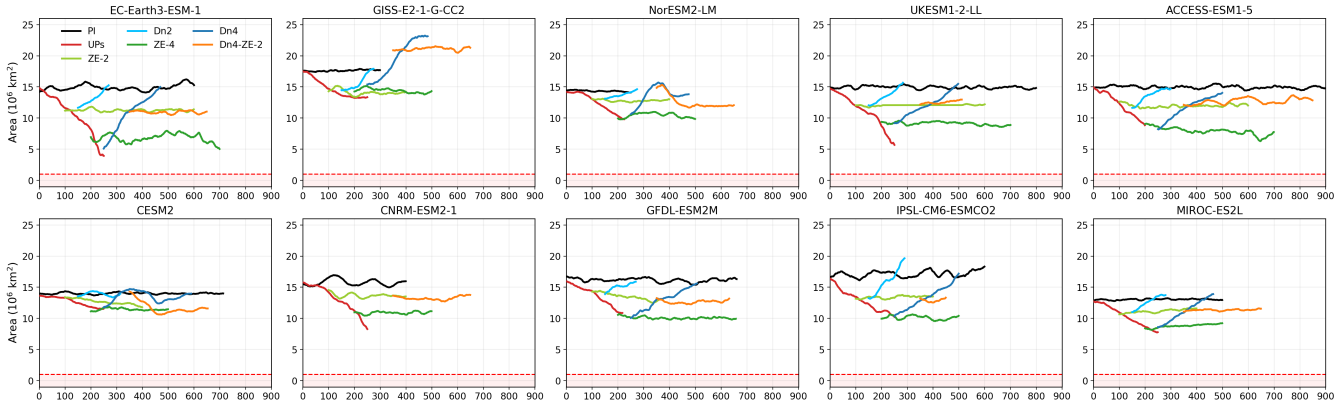

(b) **Antarctic sea ice area in September.**

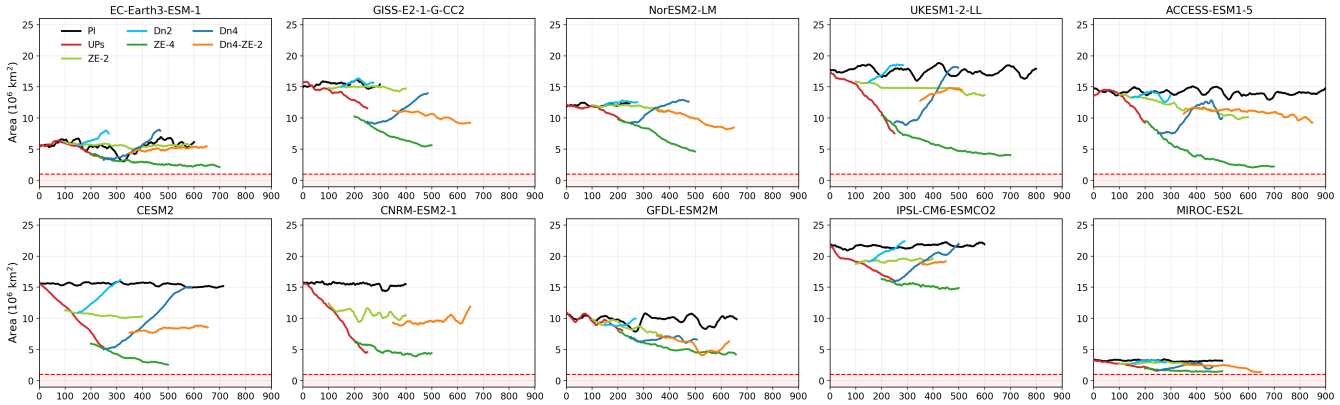

Figure S4. Winter sea ice area across TIPMIP climate pathways. (a) March Arctic sea ice area and (b) September Antarctic sea ice area for individual models across the UPs, ZE-2, ZE-4, Dn2, Dn4 and Dn4-ZE-2 experiments. Details as in Fig. S3.

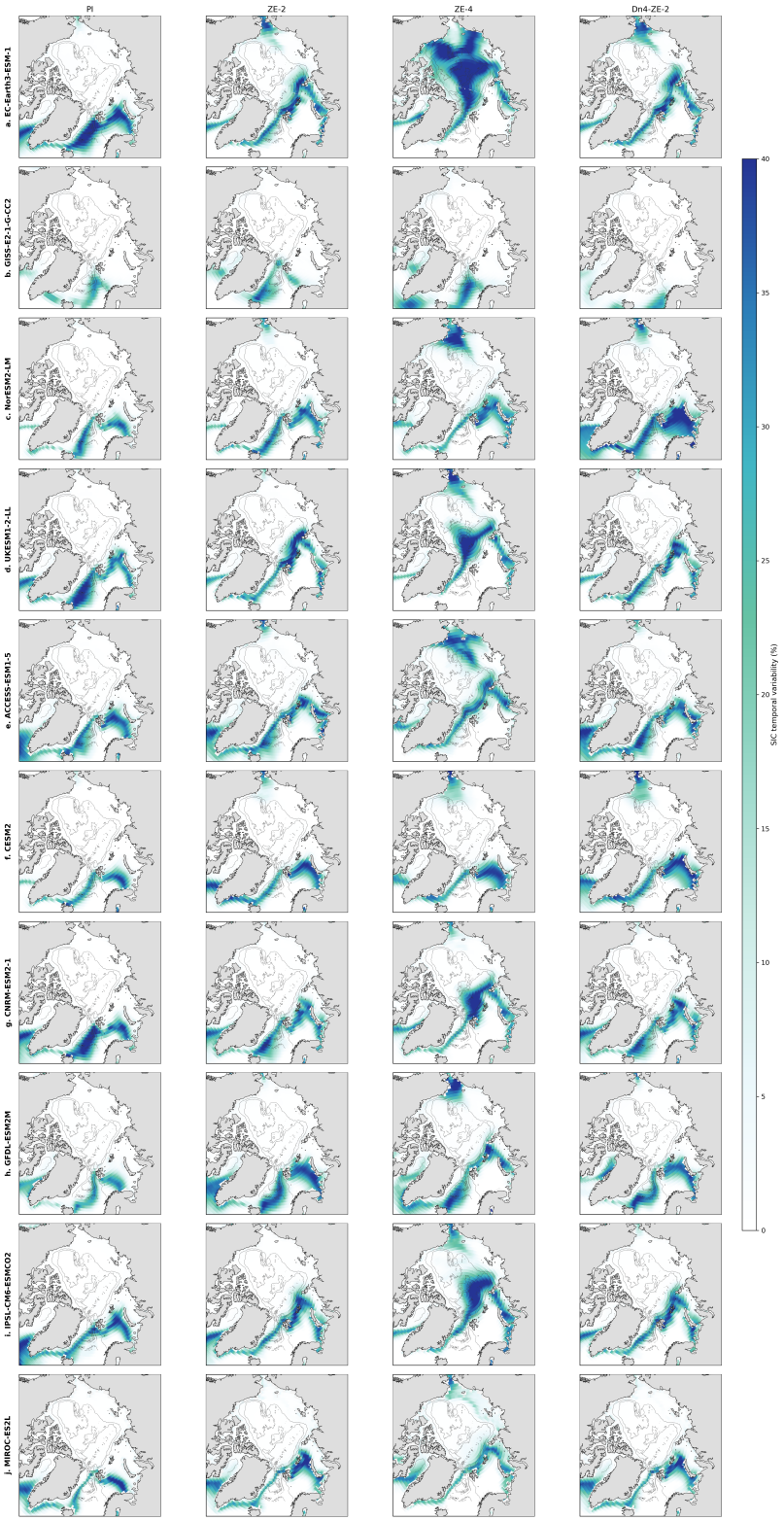

Figure S5. Model-by-model SIC variability. Arctic winter: temporal standard deviation of SIC (%) over the first 300 years of PI, ZE-2, ZE-4 and Dn4-ZE-2 for individual models.

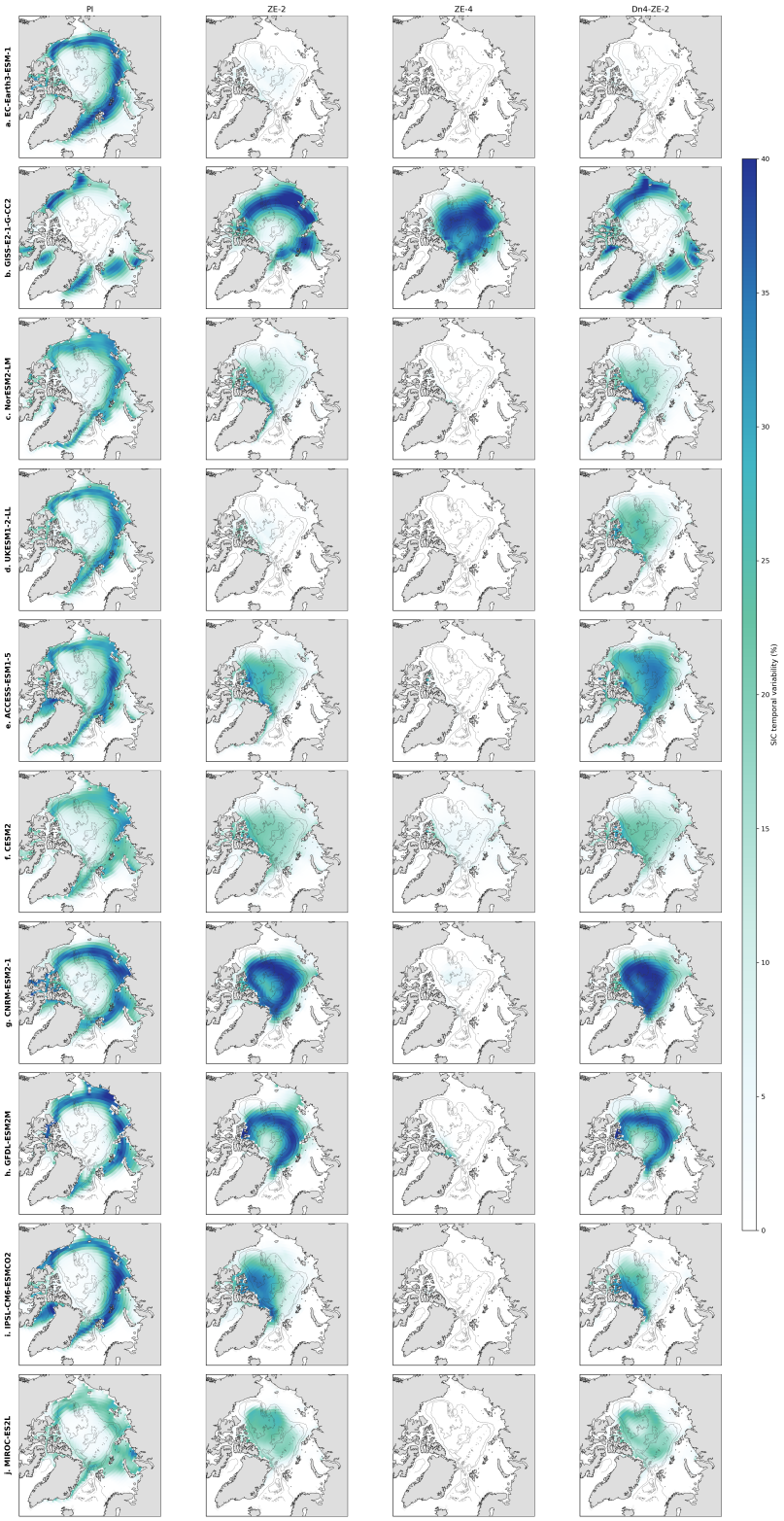

Figure S6. As Fig. S5, but for Arctic summer.

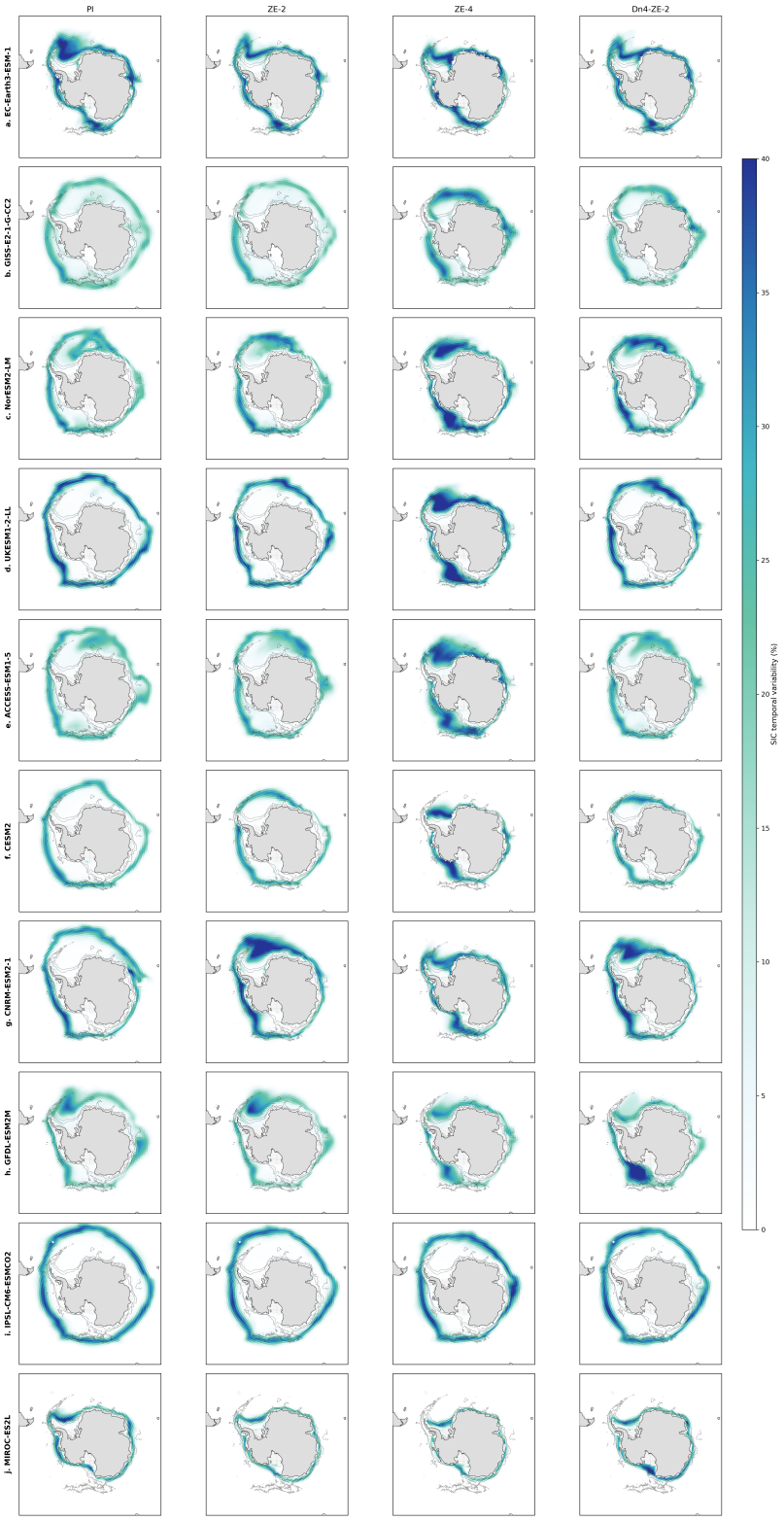

Figure S7. As Fig. S5, but for Antarctic winter.

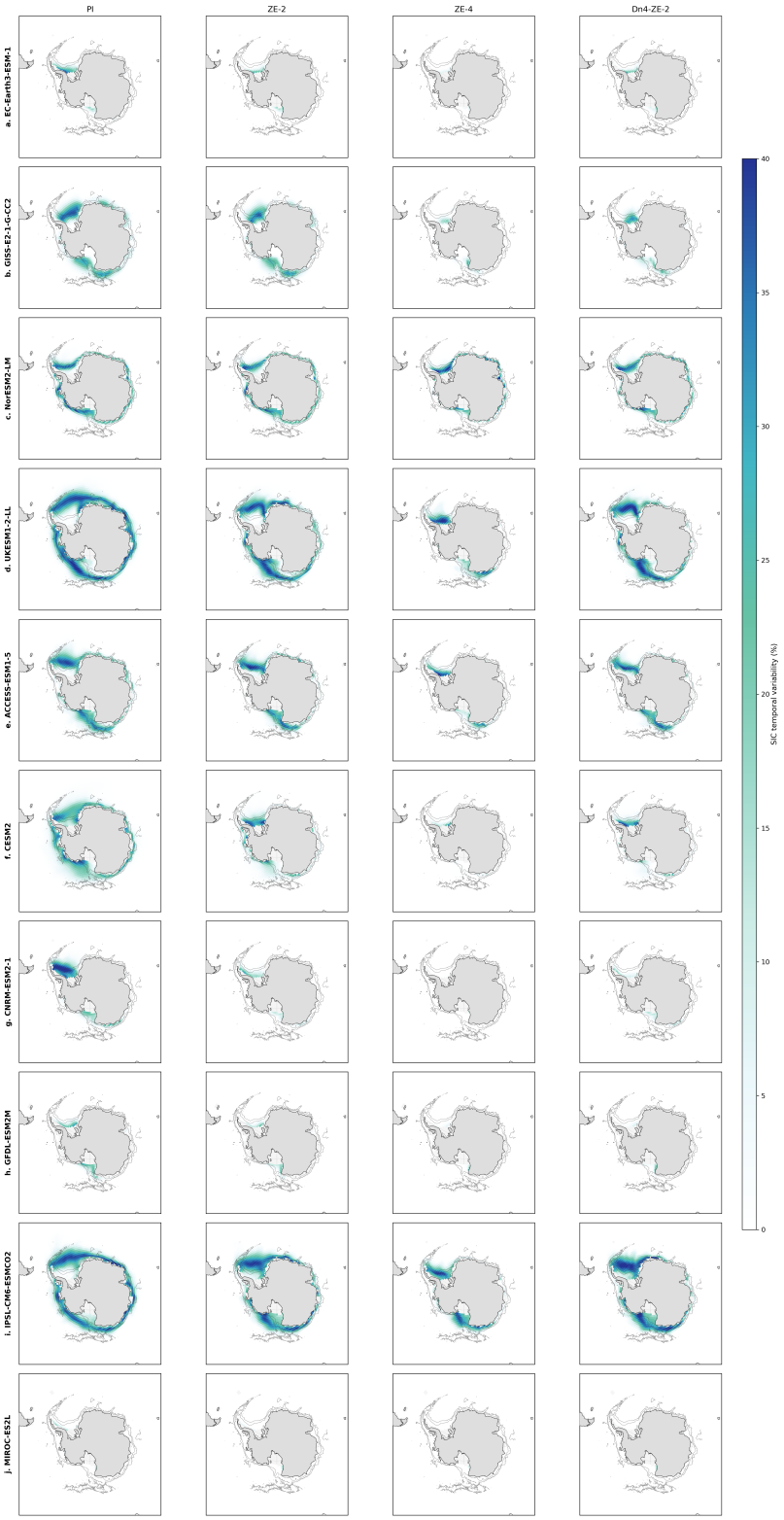

Figure S8. As Fig. S5, but for Antarctic summer.

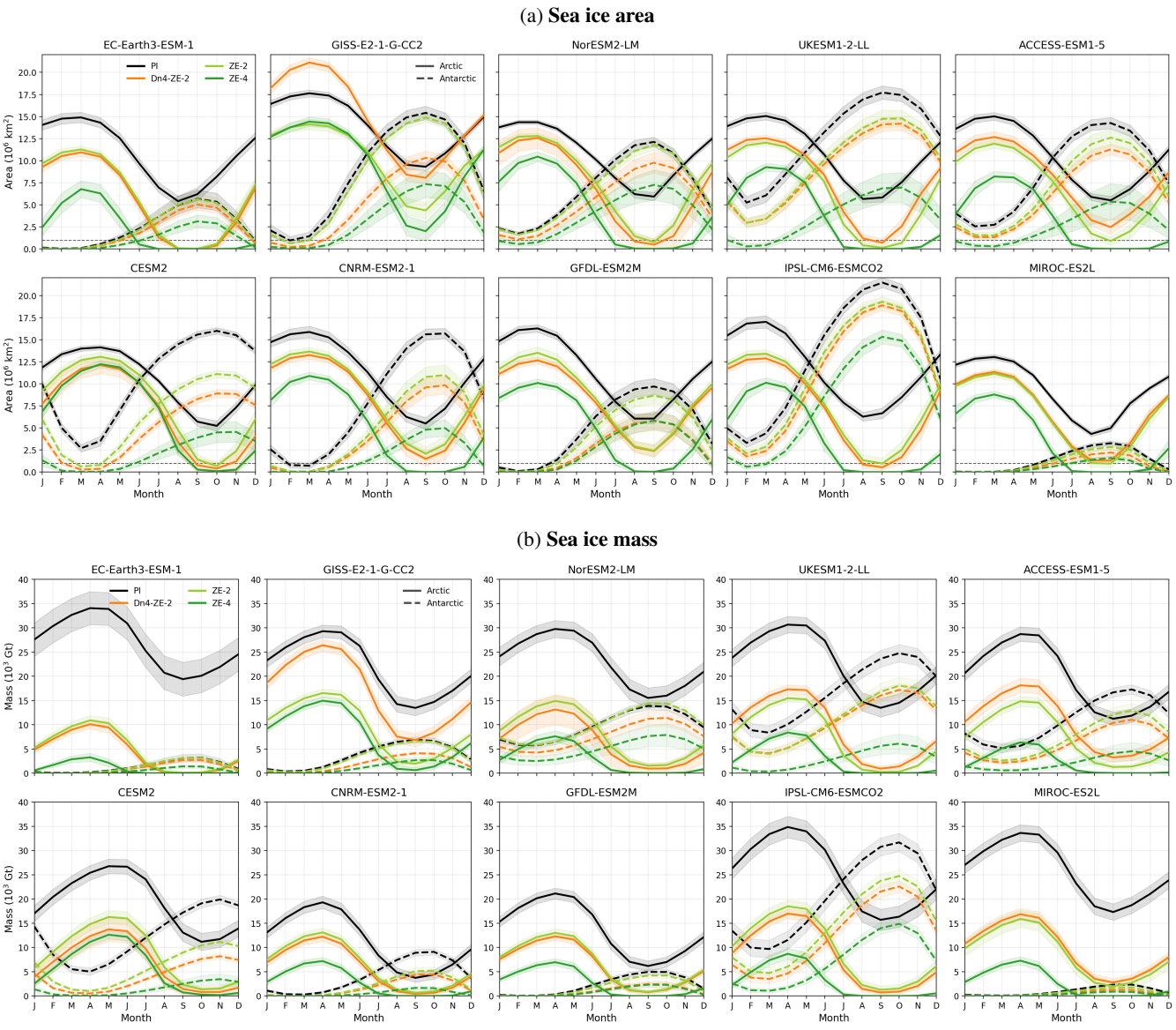

Figure S9. Model-by-model seasonal cycles of polar sea ice area and mass. Monthly climatologies of sea ice area and sea ice mass for individual models in PI, ZE-2, ZE-4 and Dn4-ZE-2. Solid and dashed lines denote the Arctic and Antarctic, respectively. Colours indicate experiments: PI (black), Dn4-ZE-2 (orange), ZE-2 (light green) and ZE-4 (dark green). Lines show the climatological monthly mean, and shading denotes the temporal standard deviation over the first $\min(300, \text{available})$ years of each experiment.

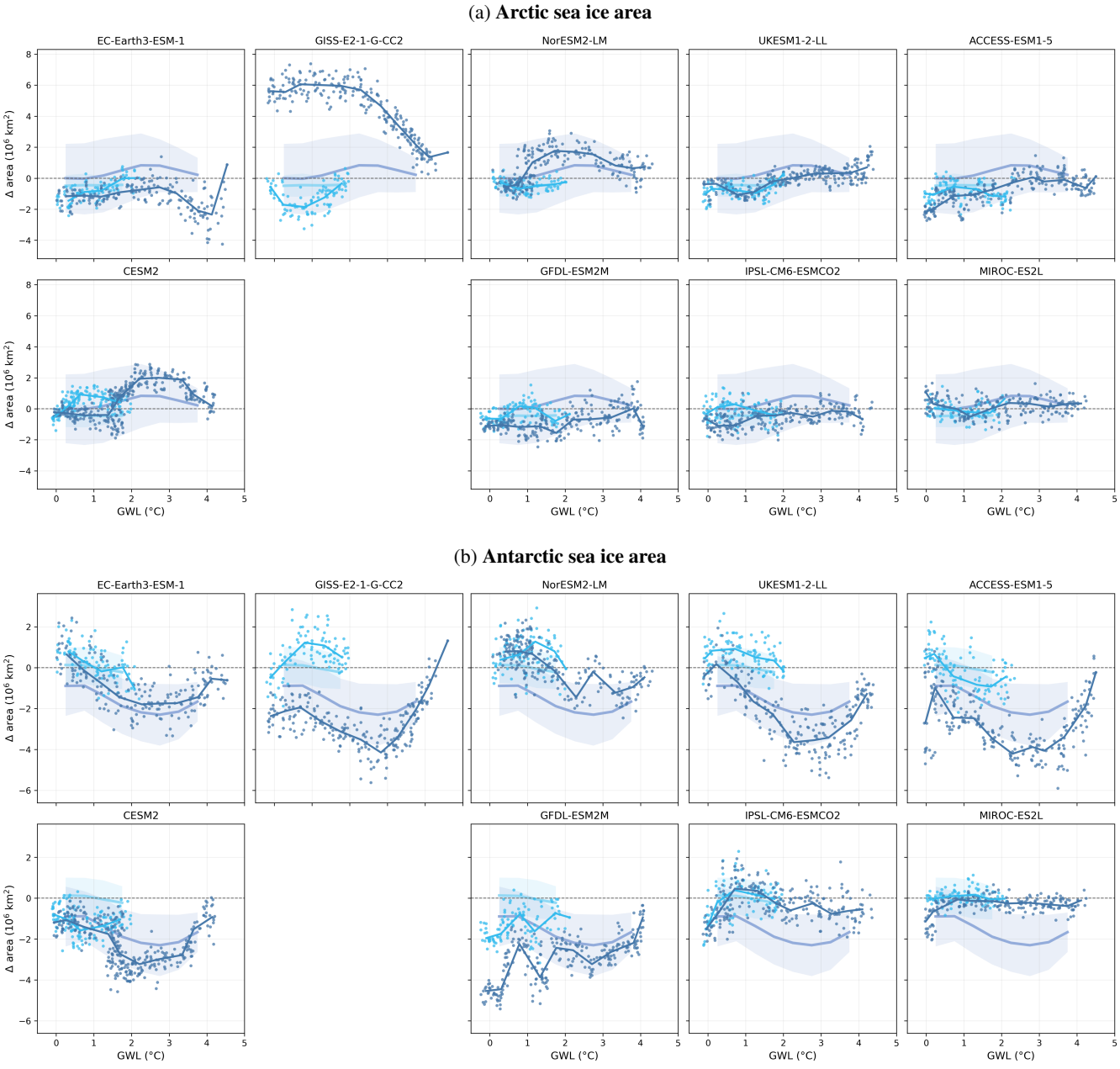

Figure S10. Model-by-model matched-GWL hysteresis in sea ice area. Hysteresis is defined as differences in sea ice area between the Dn2 and Dn4 cooling branches and the ramp-up branch at matched GWLs. Blue points and lines show individual model-matched differences, while the background thick lines and shading indicate the multi-model mean and ± 1 standard deviation. Negative values indicate lower sea ice area on the cooling branch than on the ramp-up branch at the same GWL.

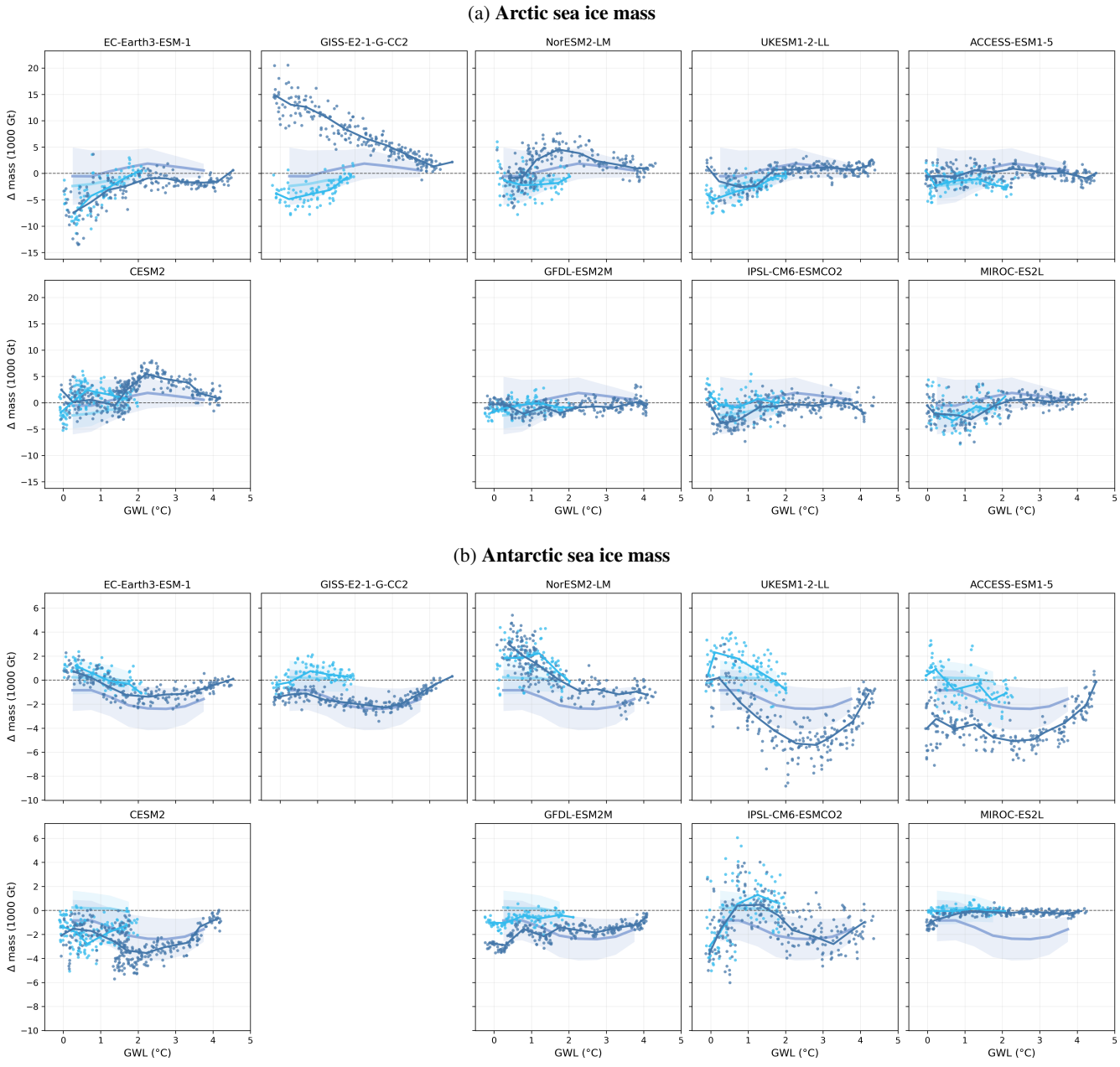

Figure S11. Model-by-model matched-GWL hysteresis in sea ice mass. As in Fig. S10, but for sea ice mass.